

IX.2 Rayleigh–Bénard convection

A relatively simple example of flow in which thermal effects play a major role is that of a fluid with a positive⁽⁵⁷⁾ thermal expansion coefficient $\alpha_{(v)}$ between two horizontal plates at constant but different temperatures, the lower plate being at the higher temperature, in a uniform gravitational potential $-\vec{\nabla}\Phi(t, \vec{r}) = \vec{g}$, in the absence of horizontal pressure gradient.

The distance between the two plates will be denoted by d , and the temperature difference between them by ΔT , with $\Delta T > 0$ when the lower plate is warmer. When needed, a system of Cartesian coordinates will be used, with the (x, y) -plane midway between the plates and a vertical z -axis, with the acceleration of gravity pointing towards negative values of z , i.e. $\Phi(t, \vec{r}) = gz$.

IX.2.1 Phenomenology of the Rayleigh–Bénard convection

IX.2.1 a Experimental findings

If both plates are at the same temperature or if the upper one is warmer ($\Delta T < 0$), the fluid between them can simply be at rest, with a stationary linear temperature profile.

⁽⁵⁷⁾This is the “usual” behavior, but there famously exist fluids with a density anomaly, like liquid water below 4°C.

As a matter of fact, denoting by T_0 resp. \mathcal{P}_0 the temperature resp. pressure at a point at $z = 0$ and ρ_0 the corresponding mass density, one easily checks that equations (IX.8), (IX.12), (IX.13) admit the static solution

$$\vec{v}_{\text{st.}}(t, \vec{r}) = \vec{0}, \quad \Theta_{\text{st.}}(t, \vec{r}) = -\frac{z}{d}\Delta T, \quad \mathcal{P}_{\text{eff.,st.}}(t, \vec{r}) = \mathcal{P}_0 - \rho_0 g \frac{z^2}{2d} \alpha_{(v)} \Delta T, \quad (\text{IX.14})$$

with the pressure given by $\mathcal{P}_{\text{st.}}(t, \vec{r}) = \mathcal{P}_{\text{eff.,st.}}(t, \vec{r}) - \rho_0 g z$. Since $|z/d| < \frac{1}{2}$ and $|\alpha_{(v)} \Delta T| \ll 1$, one sees that the main part of the pressure variation due to gravity is already absorbed in the definition of the effective pressure.

If $\Delta T = 0$, one recognizes the usual linear pressure profile of a static fluid at constant temperature in a uniform gravity field.

One can check that the fluid state defined by the profile (IX.14) is stable against small perturbations of any of the dynamical fields. To account for that property, that state (for a given temperature difference ΔT) will be referred to as “equilibrium state”.

Increasing now the temperature of the lower plate with respect to that of the upper plate, for small positive temperature differences ΔT nothing happens, and the static solution (IX.14) still holds—and is still stable.

When ΔT reaches a critical value ΔT_c , the fluid starts developing a pattern of somewhat regular cylindrical domains rotating around their longitudinal, horizontal axes, two neighboring regions rotating in opposite directions. These domains in which warmer and thus less dense fluid rises on the one side while colder, denser fluid descends on the other side, are called *Bénard cells*.^(au)

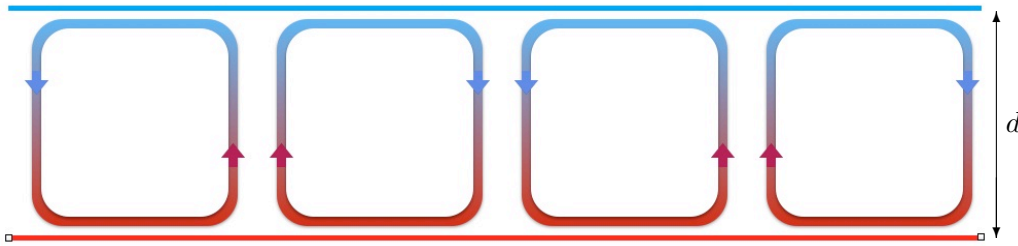


Figure IX.1 – Schematic representation of Bénard cells between two horizontal plates.

The transition from a situation in which the static fluid is a stable state, to that in which motion develops—i.e. the static case is no longer stable—is referred to as (onset of the) *Rayleigh–Bénard instability*. Since the motion of the fluid appears spontaneously, without the need to impose any external pressure gradient, it is an instance of *free convection* or *natural convection*—in opposition to *forced convection*).

Remarks:

* Such convection cells are omnipresent in Nature, as e.g. in the Earth mantle, in the Earth atmosphere, or in the Sun convective zone.

* When ΔT further increases, the structure of the convection pattern becomes more complicated, eventually becoming chaotic.

In a series of experiments with liquid helium or mercury, A. Libchaber^(av) and his collaborators observed the following features [37, 38, 39]: Shortly above ΔT_c , the stable fluid state involve cylindrical convective cells with a constant profile. Above a second threshold, “oscillatory convection” develops: that is, undulatory waves start to propagate along the “surface” of the convective cells, at first at a unique (angular) frequency ω_1 , then—as ΔT further increases—also at higher harmonics $n_1 \omega_1$, $n_1 \in \mathbb{N}$. As the temperature difference ΔT reaches a third threshold, a second undulation frequency ω_2 appears, incommensurate with ω_1 , later accompanied by the combina-

^(au)H. BÉNARD, 1874–1939. ^(av)A. LIBCHABER, born 1934

tions $n_1\omega_1 + n_2\omega_2$, with $n_1, n_2 \in \mathbb{N}$. At higher ΔT , the oscillator with frequency ω_2 experiences a shift from its proper frequency to a neighboring submultiple of ω_1 —e.g., $\omega_1/2$ in the experiments with He—, illustrating the phenomenon of *frequency locking*. For even higher ΔT , submultiples of ω_1 appear (“frequency demultiplication”), then a low-frequency continuum, and eventually chaos.

Each appearance of a new frequency may be seen as a *bifurcation*. The ratios of the experimentally measured lengths of consecutive intervals between successive bifurcations provide an estimate of the (first) *Feigenbaum constant*^(aw) in agreement with its theoretical value—thereby providing the first empirical confirmation of Feigenbaum’s theory.

IX.2.1 b Qualitative discussion

Consider the fluid in its “equilibrium” state of rest, in the presence of a positive temperature difference ΔT , so that the lower layers of the fluid are warmer than the upper ones.

If a fluid particle at altitude z acquires, for some reason, a temperature that differs from the equilibrium temperature—measured with respect to some reference value— $\Theta(z)$, then its mass density given by Eq. (IX.9) will differ from that of its environment. As a result, the Archimedes force acting on it no longer exactly balances its weight, so that it will experience a buoyancy force. For instance, if the fluid particle is warmer than its surroundings, it will be less dense and experience a force directed upwards. Consequently, the fluid particle should start to move in that direction, in which case it encounters fluid which is even colder and denser, resulting in an increased buoyancy and a continued motion. According to that reasoning, *any* vertical temperature gradient should result in a convective motion.

There are however two effects that counteract the action of buoyancy, and explain why the Rayleigh–Bénard instability necessitates a temperature difference larger than a given threshold. First, the rising particle fluid will also experience a viscous friction force from the other fluid regions it passes through, which slows its motion. Secondly, if the rise of the particle is too slow, heat has time to diffuse—by heat conduction—through its surface: this tends to equilibrate the temperature of the fluid particle with that of its surroundings, thereby suppressing the buoyancy.

Accordingly, we can expect to find that the Rayleigh–Bénard instability will be facilitated when $\alpha_{(v)}\Delta Tg$ —i.e. the buoyancy per unit mass—increases, as well as when the thermal diffusivity α and the shear viscosity ν decrease.

Translating the previous argumentation in formulas, let us consider a spherical fluid particle with radius R , and assume that it has some vertically directed velocity v , while its temperature initially equals that of its surroundings.

With the fluid particle surface area, proportional to R^2 , and the thermal diffusivity κ , one can estimate the characteristic time for heat exchanges between the particle and the neighboring fluid, namely

$$\tau_Q = C \frac{R^2}{\alpha}$$

with C a geometrical factor. If the fluid particle moves with constant velocity v during that duration τ_Q , while staying at almost constant temperature since heat exchanges remain limited, the temperature difference $\delta\Theta$ it acquires with respect to the neighboring fluid is

$$\delta\Theta = \frac{\partial\Theta}{\partial z} \delta z = \frac{\partial\Theta}{\partial z} v \tau_Q = C \frac{\Delta T}{d} \frac{R^2}{\alpha} v,$$

where $\Delta T/d$ is the vertical temperature gradient in the fluid imposed by the two plates. This temperature difference gives rise to a mass density difference

$$\delta\rho = -\rho_0 \alpha_{(v)} \delta\Theta = -C \rho_0 v \frac{R^2}{\alpha} \frac{\alpha_{(v)} \Delta T}{d},$$

^(aw)M. FEIGENBAUM, 1944–2019

between the particle and its surroundings. As a result, the fluid particle experiences an upwards directed buoyancy

$$-\frac{4\pi}{3}R^3\delta\rho g = \frac{4\pi C}{3}\rho_0 g v \frac{R^5}{\alpha} \frac{\alpha_{(v)}\Delta T}{d}. \quad (\text{IX.15})$$

On the other hand, the fluid particle is slowed in its vertical motion by the downwards oriented Stokes friction force acting on it, namely, in projection on the z -axis

$$F_{\text{Stokes}} = -6\pi R\eta v. \quad (\text{IX.16})$$

Note that assuming that the velocity v remains constant, with a counteracting Stokes force that is automatically the “good” one, relies on the picture that viscous effects adapt instantaneously, i.e. that momentum diffusion is fast. That is, the above reasoning actually assumes that the Prandtl number (IX.7) is much larger than 1; yet its result is independent from that assumption.

Comparing Eqs. (IX.15) and (IX.16), buoyancy will overcome friction, and thus the Rayleigh–Bénard instability take place, when

$$\frac{4\pi C}{3}\rho_0 g v \frac{R^5}{\alpha} \frac{\alpha_{(v)}\Delta T}{d} > 6\pi R\rho_0 \nu v \quad \Leftrightarrow \quad \frac{\alpha_{(v)}\Delta T g R^4}{\alpha \nu d} > \frac{9}{2C}.$$

Note that the velocity v that was invoked in the reasoning actually drops out from this condition. Taking for instance $R = d/2$ —which maximizes the left member of the inequality—, this becomes

$$\text{Ra} \equiv \frac{\alpha_{(v)}\Delta T g d^3}{\nu \alpha} > \frac{72}{C} = \text{Ra}_c.$$

Ra is the so-called *Rayleigh number* and Ra_c its critical value, above which the static-fluid state is unstable against perturbation and convection takes place. The “value” $72/C$ found with the above simple reasoning on force equilibrium is totally irrelevant—both careful experiments and theoretical calculations agree with $\text{Ra}_c = 1708$ for a fluid between two very large plates—, the important lesson is the existence of a threshold.

IX.2.2 Toy model for the Rayleigh–Bénard instability

A more refined—although still crude—toy model of the transition to convection consists in considering small perturbations \vec{v} , $\delta\Theta$, $\delta\mathcal{P}_{\text{eff}}$ around a static state $\vec{v}_{\text{st.}} = \vec{0}$, $\Theta_{\text{st.}}$, $\mathcal{P}_{\text{eff.,st.}}$, and to linearize the Boussinesq equations to first order in these perturbations. As shown by Eq. (IX.14), the effective pressure $\mathcal{P}_{\text{eff.,st.}}$ actually already includes a small correction, due to $\alpha_{(v)}\Delta T$ being much smaller than 1, so that we may from the start neglect $\delta\mathcal{P}_{\text{eff}}$.

To first order in the perturbations, Eqs. (IX.12), projected on the z -axis, and (IX.13) give, after subtraction of the contributions from the static solution

$$\frac{\partial v_z}{\partial t} = \nu \Delta v_z + \alpha_{(v)} \delta\Theta g, \quad (\text{IX.17a})$$

$$\frac{\partial \delta\Theta}{\partial t} - \frac{\Delta T}{d} v_z = \alpha \Delta \delta\Theta. \quad (\text{IX.17b})$$

Moving the second term of the latter equation to the right hand side increases the parallelism of this set of coupled equations. In addition, there is also the projection of Eq. (IX.12) along the x -axis, and the velocity field must obey the incompressibility condition (IX.8).

The proper approach would now be to specify the boundary conditions, namely: the vanishing of v_z at both plates—impermeability condition—, the vanishing of v_x at both plates—no-slip condition—, and the identity of the fluid temperature at each plate with that of the corresponding plate; that is, all in all, 6 conditions. By manipulating the set of equations, it can be turned into a 6th-order linear partial differential equation for $\delta\Theta$, on which the boundary conditions can be imposed.

Instead of following this long road⁽⁵⁸⁾ we refrain from trying to really solve the equations, but rather make a simple ansatz, namely $\mathbf{v}_z(t, \vec{r}) = \mathbf{v}_0 e^{\gamma t} \cos(kx)$ —which automatically fulfills the incompressibility equation, but clearly violates the impermeability conditions—, and a similar one for $\delta\Theta$, with γ a constant. Substituting these forms in Eqs. (IX.17) yields the linear system

$$\begin{aligned}\gamma \mathbf{v}_0 &= -k^2 \nu \mathbf{v}_0 + \alpha_{(\nu)} \delta\Theta_0 g &\Leftrightarrow & (\gamma + \nu k^2) \mathbf{v}_0 - g \alpha_{(\nu)} \delta\Theta_0 = 0, \\ \gamma \delta\Theta_0 &= -k^2 \alpha \delta\Theta_0 + \frac{\Delta T}{d} \mathbf{v}_0 &\Leftrightarrow & \frac{\Delta T}{d} \mathbf{v}_0 - (\gamma + \alpha k^2) \delta\Theta_0 = 0\end{aligned}$$

for the amplitudes \mathbf{v}_0 , $\delta\Theta_0$. This admits a non-trivial solution only if

$$(\gamma + \nu k^2)(\gamma + \alpha k^2) - \frac{\alpha_{(\nu)} \Delta T}{d} g = 0. \quad (\text{IX.18})$$

This is a straightforward quadratic equation for γ . It always has two real solutions, one of which is negative—corresponding to a dampened perturbation—since their sum is $-(\alpha + \nu)k^2 < 0$; the other solution may change sign since their product

$$\alpha \nu k^4 - \frac{\alpha_{(\nu)} \Delta T}{d} g$$

is positive for $\Delta T = 0$, yielding a second negative solution, yet changes sign as ΔT increases. The vanishing of this product thus signals the onset of instability. Taking for instance $k = \pi/d$ to fix ideas, this occurs at a critical Rayleigh number

$$\text{Ra}_c = \frac{\alpha_{(\nu)} \Delta T g d^3}{\alpha \nu} = \pi^4,$$

where the precise value (here π^4) is irrelevant.

From Eq. (IX.18) also follows that the growth rate of the instability is given in the neighborhood of the threshold by

$$\gamma = \frac{\text{Ra} - \text{Ra}_c}{\text{Ra}_c} \frac{\alpha \nu}{\alpha + \nu} k^2,$$

i.e. it is infinitely slow at Ra_c . This is reminiscent of a similar behavior in the vicinity of the critical point associated with a thermodynamic phase transition.

By performing a more rigorous calculation including non-linear effects, one can show that the velocity amplitude at a given point behaves like

$$\mathbf{v} \propto \left(\frac{\text{Ra} - \text{Ra}_c}{\text{Ra}_c} \right)^\beta \quad \text{with} \quad \beta = \frac{1}{2} \quad (\text{IX.19})$$

in the vicinity of the critical value, and this prediction is borne out by experiments [41]. Such a power law behavior is again reminiscent of the thermodynamics of phase transitions, more specifically here—since \mathbf{v} vanishes below Ra_c and is finite above—of the behavior of the *order parameter* in the vicinity of a critical point. Accordingly the notation β used for the exponent in relation (IX.19) is the traditional choice for the critical exponent associated with the order parameter of phase transitions.

Eventually, a last analogy with phase transitions regards the breaking of a symmetry at the threshold for the Rayleigh–Bénard instability. Below Ra_c , the system is invariant under translations parallel to the plates, while above Ra_c that symmetry is spontaneously broken.

⁽⁵⁸⁾The reader may find details in Ref. [40] Chap. II].